

Asymmetric synthesis of heterocyclic chloroamines and aziridines by enantioselective protonation of catalytically generated enamines

Liam A. McLean,^{a‡} Matthew W. Ashford,^{a‡} James W. B. Fyfe,^a Alexandra M. Z. Slawin,^a Andrew G. Leach,^b and Allan J. B. Watson^{a*}

^aEaStCHEM, School of Chemistry, University of St Andrews, North Haugh, St Andrews, KY16 9ST, Fife, U.K.

^bSchool of Health Sciences, University of Manchester, Oxford Road, Manchester, M13 9PL, U.K.

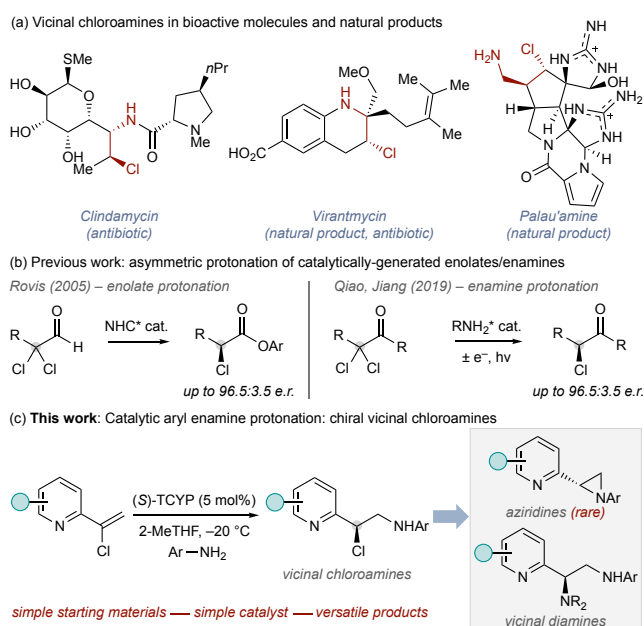
Supporting Information Placeholder

ABSTRACT: We report a method for the synthesis of chiral vicinal chloroamines via asymmetric protonation of catalytically generated prochiral chloroenamines using chiral Brønsted acids. The process is highly enantioselective, with the origin of asymmetry and catalyst substituent effects elucidated by DFT calculations. We show the utility of the method as an approach to the synthesis of a broad range of heterocycle-substituted aziridines by treatment of the chloroamines with base in a one-pot process, as well as the utility of the process to allow access to vicinal diamines.

Vicinal chloroamines are key components of natural products and pharmaceuticals (e.g., Scheme 1a) and are broadly useful intermediates for chemical synthesis.¹⁻⁷ The value of this motif has driven the development of new methodologies for their preparation, which has been largely dominated by strategies for alkene aminohalogenation.^{6,7} Asymmetric processes are of particularly high value since nucleophilic substitution allows straightforward diversification to a range of new enantioenriched carbons bearing C–heteroatom bonds. Most of these enantioselective methods use transition metal catalysis, with comparatively few examples of organocatalytic processes.⁷

To our knowledge, the formation of aryl vicinal chloroamines via organocatalytic asymmetric protonation has not been reported. There are only four reports preparing chiral carbons with C–Cl bonds via enantioselective protonation, all of which generate α -chlorocarbonyl products.⁸⁻¹¹ Of these, only two proceed via asymmetric protonation of a catalytically generated species (Scheme 1b). Rovis employed NHC catalysis for the synthesis of α -chloroacids.⁹ Qiao and Jiang used similar starting materials to generate α -chloro ketones using dual amine/photoredox catalysis.¹¹ This latter process represents the only example of an enantioselective protonation of a catalytically generated prochiral chloroenamine.^{12,13}

Here we report the development of a new approach for the synthesis of chiral carbons bearing C–Cl bonds via enantioselective protonation of catalytically generated prochiral chloroenamines (Scheme 1c). This process allows simultaneous formation of a new C–N bond and generation of a new Cl-substituted stereogenic centre under simple reaction conditions, providing access to vicinal chloroamines.



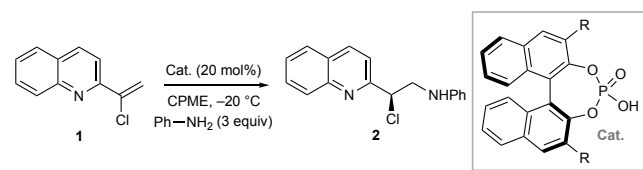
Scheme 1. (a) Examples of vicinal chloroamines. (b) Previous work: catalytic enolate/enamine protonation. (c) This work: catalytic chloroenamine protonation – access to heterocyclic chloroamines, aziridines, and diamines.

Only three examples of catalytic asymmetric synthesis of heterocycle-substituted aziridines have been reported,¹⁴⁻¹⁶ and all of these prepare the same product. This new strategy therefore simultaneously addresses a limitation in aziridination methodologies, while also allowing access to diamines.

A benchmark system using chlorovinyl quinoline **1** and aniline was used for reaction development (Table 1). An initial screening campaign identified promising conditions using 20 mol% catalyst **3** at -20 °C in CPME (Entry 1; for full screening details, see Tables S1-S6).^{17,18} However, further attempts at reaction optimization did not improve asymmetric induction. We therefore conducted an extensive catalyst screen (see Table S1), which, in combination with DFT analysis (*vide infra*), allowed catalyst SAR to be rationalized and provided insight into substituent effects more broadly. The parent, unsubstituted BINOL catalyst **4** delivers low enantioselectivity (entry 2), as expected from prior work in this field.¹⁹ Systematic exploration of the aryl groups at the 3,3'-substituents to understand the selectivity determinants of catalyst **3** was informative. As expected,¹⁹ 3,3'-

diphenyl catalyst **5** delivered improvement upon the enantioselectivity offered by unsubstituted catalyst **4** (entry 3). However, introduction of an *i*-Pr group at the 4-position of the 3,3'-aryl units (**6**) had no effect on enantioselectivity (entry 4), suggesting this position has very little effect on enantiofacial discrimination.

Table 1. Reaction development.



Entry	R (Catalyst)	2 (%) (e.r.) ^a
1	2,4,6-(<i>i</i> -Pr) ₃ C ₆ H ₂ (3)	98% (90:10)
2	H (4)	90% (51:49)
3	Ph (5)	71% (64:36)
4	4-(<i>i</i> -Pr)C ₆ H ₄ (6)	97% (67:33)
5	3,5-(<i>i</i> -Pr) ₂ C ₆ H ₃ (7)	73% (74:26)
6	3,5-(<i>t</i> -Bu) ₂ C ₆ H ₃ (8)	70% (71:29)
7	2,6-(<i>i</i> -Pr) ₂ C ₆ H ₃ (9)	77% (88:12)
8	2,4,6-(<i>c</i> -Pent) ₃ C ₆ H ₂ (10)	95% (90:10)
9	2,4,6-(<i>c</i> -Hex) ₃ C ₆ H ₂ (11)	96% (96:4)
10	2,4,6-(<i>c</i> -Hept) ₃ C ₆ H ₂ (12)	95% (97:3)
11^b	2,4,6-(c-Hex)₃C₆H₂ (11)	96% (97:3)

^a Determined by HPLC analysis. ^b Reaction conditions: **11** (5 mol%), 2-MeTHF, PhNH₂ (1 equiv).

Selectivity increased marginally by moving the *i*-Pr groups to the 3,5-positions (**7**, entry 5); however, selectivity remained significantly lower than for **3** even when the steric component was increased, for example, with *t*-Bu-substituted catalyst **8** (entry 6). These data suggested the 3-,4-, and 5-positions of the 3,3' aryl units exert a weak influence on stereoselectivity. This was compounded by assessment of catalyst **9**, which lacks the 4-(*i*-Pr) unit yet delivers approximately the same enantioinduction as **3** (entry 7 vs. entry 1). The lower importance of the 3-, 4-, and 5-positions of the aryl unit was further supported by assessment of a range of functional groups at these positions on the BINOL scaffold as well as in alternative catalyst frameworks (Table S1). However, while having little to no effect on enantioinduction, the 4-position of these aryl units was found to directly affect reactivity: increased conversion (*ca.* 20%) to product was observed for those catalysts with 4-*i*-Pr compared to those without (**5** vs. **6**, **9** vs. **3**).

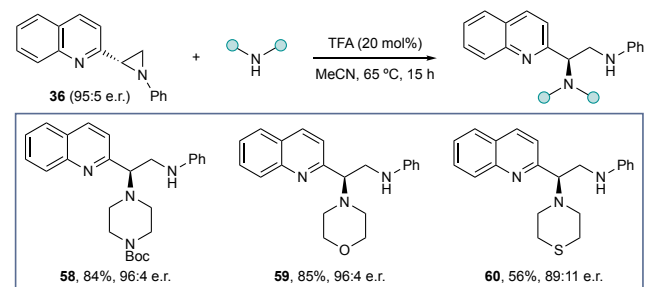
Second phase catalyst screening revealed the introduction of cycloalkyl groups to the 3,3' aryl units improved enantioselectivity while remaining synthetically tractable. *c*-Pent derivative **10**²⁰ was found to be equivalent to *i*-Pr catalyst **3** (entry 8); however, *c*-Hex catalyst **11** (TCYP),²¹ and *c*-Hept catalyst **12** (entry 10) provided marked improvement, with **11** subsequently offering excellent reactivity and selectivity at 5 mol% loading and equimolar PhNH₂ in 2-MeTHF (entry 11).

The reaction conditions identified in entry 11 were assessed for generality by application towards the synthesis of a range of vicinal chloroamines (Scheme 2a). Broad variation of the aniline nucleophile was generally accommodated, delivering the expected chloroamines in good yield and with high enantioselectivity throughout; however, **17** was noted as a clear exception, providing racemic product, which could be related to the

pK_a of this specific aniline. Confirmation of product stereochemistry was achieved by crystallization of **20**, which also highlighted the solid-state conformational preferences of the chloroamine, where the C–Cl is *gauche* to both nitrogen atoms. Variation of the azaheterocycle was also generally successful (**26–35**), although significant variation in reactivity was noted and driven by changes in heteroaryl electronics. Other *N*-nucleophiles (e.g., alkyl amines) were not tolerated in this process due to competing protonation events.

As noted above, this approach to vicinal chloroamines can allow access to rare heterocycle-substituted aziridines (Scheme 2b). Following the asymmetric protonation process, *in situ* treatment of the chloroamine with base delivered a library of products **36–53**. Variation in the *N*-aryl component was straightforward, with structural data of complementary product **44** (100% *es*) confirming the absolute stereochemistry. Variation of the *N*-heterocycle was also tolerated; however, in this case the observed variation in reaction efficiency was due to the stability of the aziridine products, several of which were found to be particularly reactive and unstable to isolation (e.g., **54–57**). In addition, the S_Ni event was found to have high solvent dependency: a solvent switch was necessary for **51** and **53** where THF led to completely racemic products, presumably through a more ionic pathway, where toluene allowed for exclusive S_Ni.

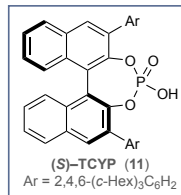
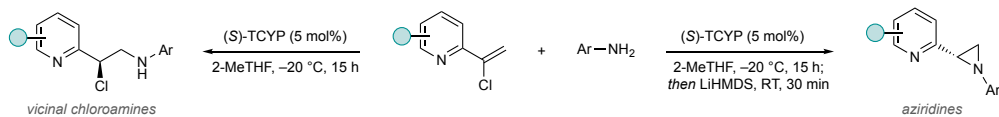
Access to the aziridine products above allows further derivatization. For example, heterocyclic vicinal diamines are also relatively rare chemotypes. However, these can be prepared by treatment of the heterocyclic aziridines with, for example, a cyclic amine in the presence of catalytic TFA giving **58–60** with high fidelity for S_N2 at the benzylic stereocenter (Scheme 3).



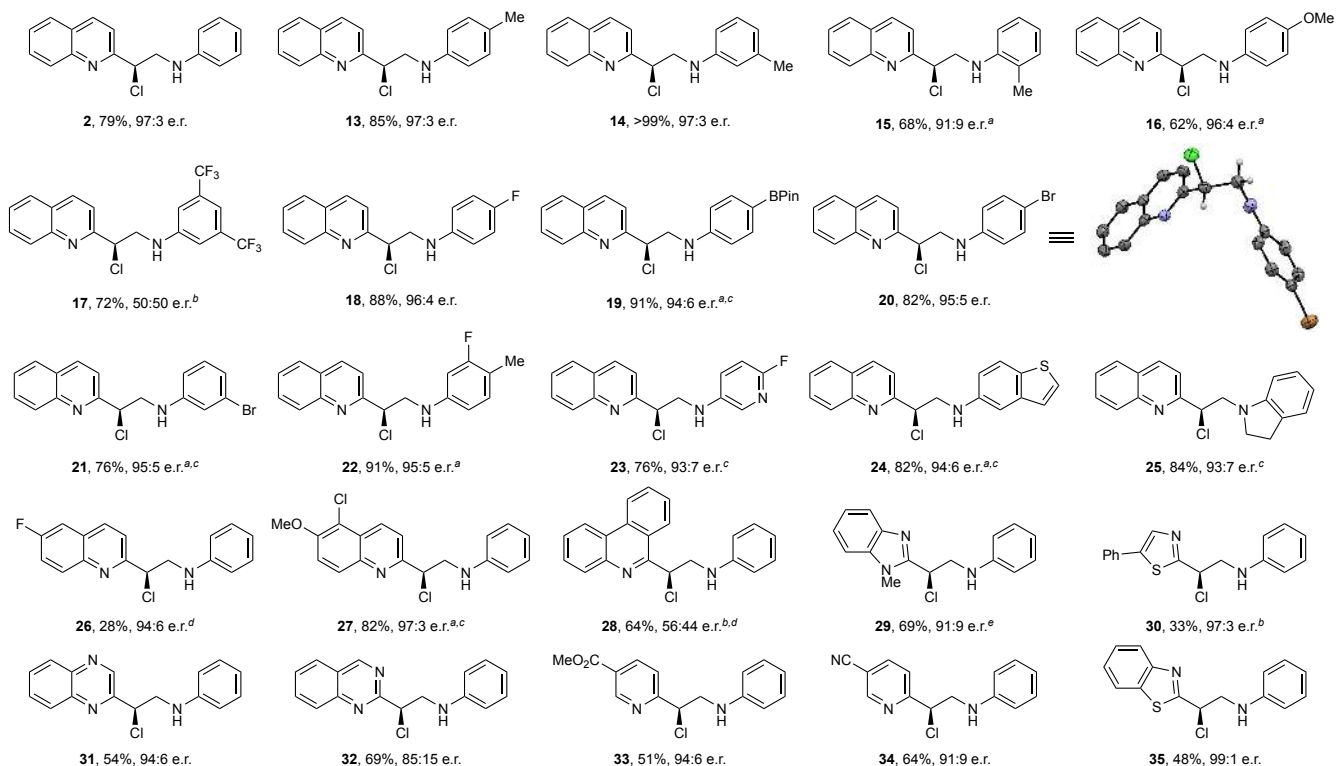
Scheme 3. Synthesis of heterocyclic vicinal diamines.

To gain greater insight into catalyst SAR and rationalize the superior selectivity observed using TCYP (**11**) vs. TRIP (**3**), we undertook an in-depth computational evaluation of the system using the ONIOM method with B3LYP/6-31G**²² for the QM region and UFF²³ for the MM region.²⁴ Calculations were performed using Gaussian09 (see SI).^{17,18,25}

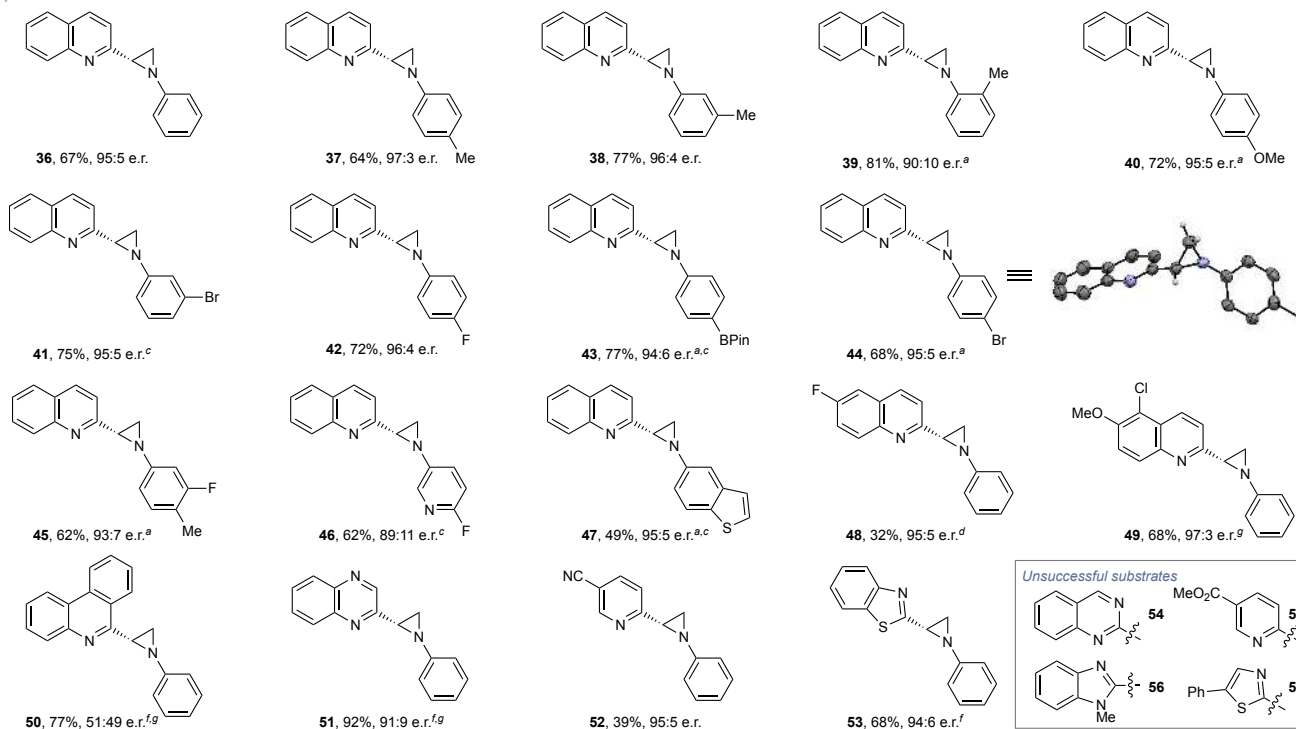
A reaction profile for TRIP catalyst (**3**) is shown in Figure 1 (for full analysis, see SI). Benchmark substrate **1** preferentially adopts the lower energy *s-trans* conformation (2.2 kcal/mol preferred vs. *s-cis*; Figure S2). Consistent with our previous model,^{17,18} the reaction proceeds through (1) complexation of **1** with **3** via a hydrogen bond to give **61**, (2) nucleophilic addition of aniline, via **62**, to the catalyst-substrate complex and proton transfer back to the catalyst to yield **63** (3) protonation of this prochiral enamine by the catalyst via **64**, and (4) product dissociation. From a free energy perspective, the aniline addition and proton transfer to the catalyst form a concerted process leading to **63**.



(a) Vicinal chloroamines



(b) Aziridines



Scheme 2. (a) Example scope of the chloroamine process. (b) Example scope of the aziridination process. Isolated yields. Enantiomeric ratios determined by HPLC analysis. ^a 39 h; ^b RT; ^c CPME; ^d 4 days; ^e 0 °C; ^f PhMe; ^g Accessed from isolated chloroamine.

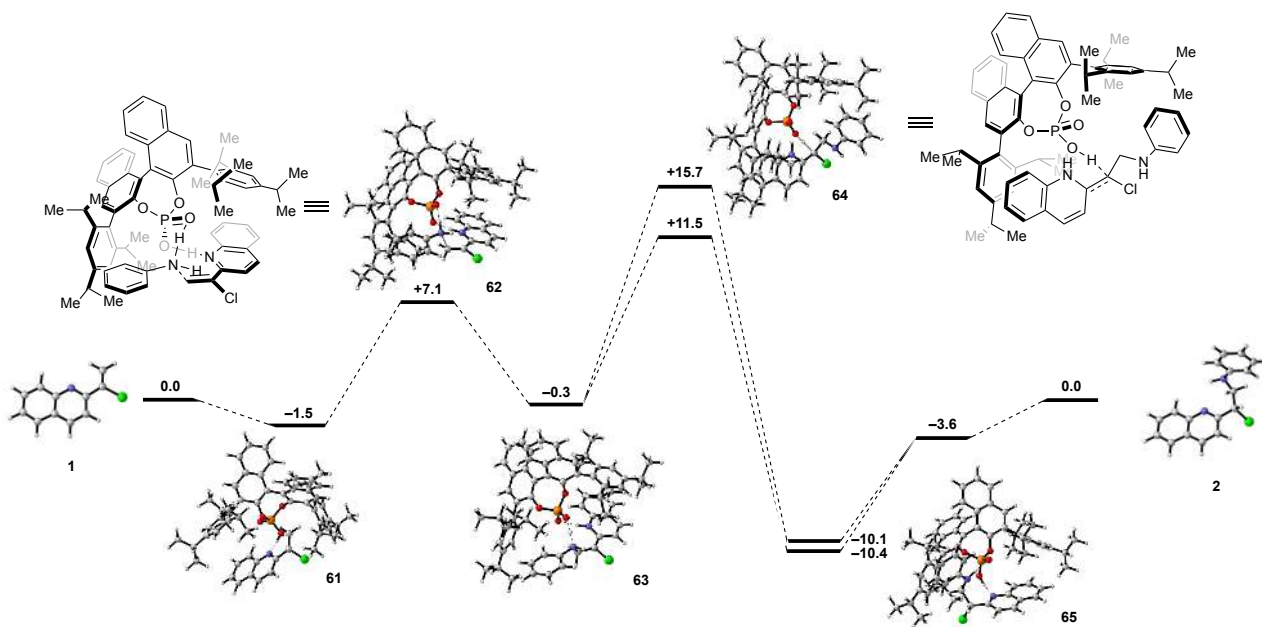


Figure 1. Reaction mechanism using **1** and catalyst **3**. Energies in kcal mol⁻¹

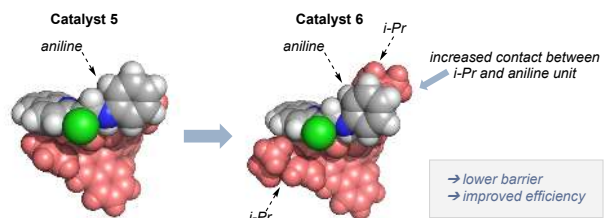
For the TRIP-catalyzed process, the pathway to the experimentally obtained (*R*)-enantiomer is favored by *ca.* 4 kcal/mol in agreement with the experimentally observed enantiomer.

Computational modelling assisted in rationalizing the reactivity and stereoselectivity SAR observed during catalyst screening reported in Table 1 (Figure 2a). Free energy barriers for the catalytic cycle are lower for catalysts possessing the 4-(*i*-Pr) group (**3** and **6**) than for those without (**5**) or for the catalyst with 3,5-substituents (**7**, **8**; Table S8, S10). The overall barrier arises from a combination of how effectively the catalyst stabilizes the ground state (the catalyst-product complex (**65**, Figure 1)) and the reaction transition state (**64**, Figure 1). The inclusion of a 4-(*i*-Pr) group to catalyst **5** gives catalyst **6**. This increases substrate-catalyst interactions, decreasing ground state stabilization more than the corresponding effect on the transition state, leading to a reduction in barrier. In contrast, adding *i*-Pr groups at positions 3 and 5 (catalyst **7**) causes an even larger destabilization of the ground state; however, this is exceeded by the effect on the transition state, leading to an overall increase in energy barrier. For **6**, the disruption of aromatic stacking in the product complex **65** is outweighed by added van der Waals-type contacts in the transition state **64** (*vide infra*) while this does not happen for **7**.

Similar effects are responsible for the increased enantioselectivity offered by catalysts **10-12** in comparison to **3** (e.g., Figure 2b for comparison of **3** vs. **11**). Catalyst-transition state complex **64** adopts a preferred conformation where the C-Cl bond is *anti* with respect to the catalyst P=O (Figure S7) and this is not possible for the pro-*S* transition state due to the 3,3'-substituents: this is a key contributor to enantioselectivity. In the alternative conformation that must be adopted when the catalyst has a 3,3'-substituent, the aniline unit adopts an *anti*-orientation that places it between two of the 2,6-alkyl substituents: these are then key to enantioselectivity in the rate-determining proton transfer event. As the substituent bulk is increased from *i*-Pr (catalyst **3**) to cycloalkyl (catalysts **10-12**), transition state-stabilizing contacts increase between the alkyl group at the 4-

position and the aniline unit in the favored transition state. This serves to strengthen preference for the observed enantiomer. In contrast, moving from *i*-Pr to larger cycloalkyl groups increasingly destabilizes the transition state that leads to the disfavored enantiomer by compressing the gap that the aniline occupies – the aniline is effectively extruded and must rotate away.

(a) Increased contacts of the 4-(*i*-Pr) group – improved reaction efficiency



(b) Shape complementarity of cycloalkyl unit – improved selectivity

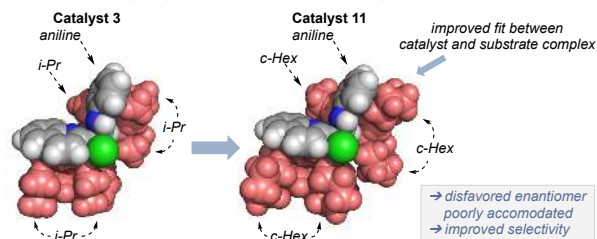


Figure 2. Space-filling models of the effect of (a) the 4-(*i*-Pr) group and (b) cycloalkyl groups.

Thus, good shape complementarity with the 4-alkyl in the pro-*R* transition state and space-filling by the 2,6-alkyl groups in the pro-*S* transition state lead to the observed improvement in enantioselectivity with the cycloalkyl catalysts.

In summary, a method for the synthesis of chiral heterocyclic vicinal chloroamines has been developed. The reaction relies upon asymmetric protonation of a catalytically generated aryl chloroamine using a chiral Brønsted acid and represents the first example of this process. A range of chloramine products can be accessed and, in turn, provide access to rare heterocyclic

aziridines and diamines, bridging a significant gap in synthetic methodologies for the preparation of these product classes. Computational analysis has assisted in rationalizing observations of increased reactivity and enantioselectivity with cycloalkyl CPA catalysts, providing insight into the specific function of these alkyl units in these processes.^{26,27}

ASSOCIATED CONTENT

AUTHOR INFORMATION

Corresponding Author

*aw260@st-andrews.ac.uk

Author Contributions

‡These authors contributed equally.

Funding Sources

No competing financial interests have been declared.

EPSRC grant number EP/S027165/1

EPSRC grant number EP/R025754/1

Leverhulme Trust grant number RPG-2018-362

ACKNOWLEDGMENT

L.A.M. and J.W.B.F. thank EPSRC for postdoctoral funding (EP/S027165/1; EP/R025754/1). J.W.B.F. thanks the Leverhulme Trust for postdoctoral funding (RPG-2018-362). M.W.A. thanks the University of St Andrews for a PhD studentship. A.G.L. would like to acknowledge the assistance given by Research IT and the use of the Computational Shared Facility at The University of Manchester.

REFERENCES

- (1) Nakagawa, A.; Iwai, Y.; Hashimoto, H.; Miyazaki, N.; Oiwa, R.; Takahashi, Y.; Hirano, A.; Shibukawa, N.; Kojima, Y.; Omura, S. Virantmycin, A New Antiviral Antibiotic Produced by a Strain of *Streptomyces*. *J. Antibiot.* **1981**, *34*, 1408–1415.
- (2) Nakamura, H.; Ohizumi, Y.; Kobayashi, J.; Hirata, Y. Keramide, A Novel Antagonist of Serotonergic Receptors Isolated from the Okinawan Sea Sponge *Agelas sp. Tetrahedron Lett.* **1984**, *25*, 2475–2478.
- (3) Kinnel, R. B.; Gehrken, H.-P.; Scheuer, P. J. Palau'amine: A Cytotoxic and Immunosuppressive Hexacyclic Bisguanidine Antibiotic from the Sponge *Stylotella agminata*. *J. Am. Chem. Soc.* **1993**, *115*, 3376–3377.
- (4) Qiu, J.; Silverman, R. B. A New Class of Conformationally Rigid Analogues of 4-Amino-5-halopentanoic Acids, Potent Inactivators of γ -Aminobutyric Acid Aminotransferase. *J. Med. Chem.* **2000**, *43*, 706–720.
- (5) Gribble, G. W. *Occurrence of Halogenated Alkaloids*. In *The Alkaloids*; Academic Press: New York, 2012; Vol. 71, Chapter 1.
- (6) Li, G.; Kotti, S. R. S. S.; Timmons, C. Recent Development of Regio- and Stereoselective Aminohalogenation Reaction of Alkenes. *Eur. J. Org. Chem.* **2007**, 2745–2758.
- (7) Chemler, S. R.; Bovino, M. T. Catalytic Aminohalogenation of Alkenes and Alkynes. *ACS Catalysis* **2013**, *6*, 1076–1091.
- (8) Nakamura, S.; Kaneeda, M.; Ishihara, K.; Yamamoto, H. Enantioselective Protonation of Silyl Enol Ethers and Ketene Disilyl Acetals with Lewis Acid-Assisted Chiral Brønsted Acids: Reaction Scope and Mechanistic Insights. *J. Am. Chem. Soc.* **2000**, *122*, 8120–8130.
- (9) Reynolds, N. T.; Rovis, T. Enantioselective Protonation of Catalytically Generated Chiral Enolates as an Approach to the Synthesis of α -Chloroesters. *J. Am. Chem. Soc.* **2005**, *127*, 16406–16407.
- (10) Uraguchi, D.; Kizu, T.; Ohira, Y.; Ooi, T. Enantioselective Protonation of α -Hetero Carboxylic Acid-derived Ketene Disilyl Acetals Under Chiral Ionic Brønsted Acid Catalysis. *Chem. Commun.* **2014**, *50*, 13489–13491.
- (11) Hou, M.; Lin, K.; Chai, X.; Zhao, X.; Qiao, B.; Jiang, Z. Enantioselective Photoredox Dehalogenative Protonation. *Chem. Sci.* **2019**, *10*, 6629–6634.
- (12) Diastereoselective processes are well known. For example, see: (a) Wang, Y.; Liu, X.; Deng, L. Dual-Function Cinchona Alkaloid Catalysis: Catalytic Asymmetric Tandem Conjugate Addition-Protonation for the Direct Creation of Nonadjacent Stereocenters. *J. Am. Chem. Soc.* **2006**, *128*, 3928–3930. (b) Wang, B.; Wu, F.; Wang, Y.; Liu, X.; Deng, L. Control of Diastereoselectivity in Tandem Asymmetric Reactions Generating Nonadjacent Stereocenters with Bifunctional Catalysis by Cinchona Alkaloids. *J. Am. Chem. Soc.* **2007**, *129*, 768–769.
- (13) An enantioselective chloroamine protonation has been proposed as a possible pathway in chiral amine-catalyzed α -chlorination of aldehydes. See: Burés, J.; Armstrong, A.; Blackmond, D. G. *J. Am. Chem. Soc.* **2012**, *134*, 6741–6750.
- (14) Gupta, A. K.; Mukherjee, M.; Wulff, W. D. Multicomponent Catalytic Asymmetric Aziridination of Aldehydes. *Org. Lett.* **2011**, *13*, 5866–5869.
- (15) Mukherjee, M.; Zhou, Y.; Gupta, A. K.; Guan, Y.; Wulff, W. D. A General Synthesis of Sphingamines through Multicomponent Catalytic Asymmetric Aziridination. *E. J. Org. Chem.* **2014**, 1386–1390.
- (16) Bew, S. P.; Liddle, J.; Hughes, D. L.; Pesce, P.; Thurston, S. M. Chiral Brønsted Acid-Catalyzed Asymmetric Synthesis of *N*-Aryl-*cis*-aziridine Carboxylate Esters. *Angew. Chem. Int. Ed.* **2017**, *56*, 5322–5326.
- (17) Xu, C.; Muir, C. W.; Leach, A. G.; Kennedy, A. R.; Watson, A. J. B. Catalytic Enantioselective Synthesis of Chiral Azaheterocyclic Ethylamines by Asymmetric Protonation. *Angew. Chem. Int. Ed.* **2018**, *57*, 11374–11377.
- (18) Ashford, M. W.; Xu, C.; Molloy, J. J.; Carpenter-Warren, C.; Slawin, A. M. Z.; Leach, A. G.; Watson, A. J. B. Catalytic Enantioselective Synthesis of Heterocyclic Vicinal Fluoroamines Using Asymmetric Protonation: A Method Development and Mechanistic Study. *Chem. Eur. J.* **2020**, *26*, 12249–12255.
- (19) (a) Akiyama, T.; Mori, K. Stronger Brønsted Acids: Recent Progress. *Chem. Rev.* **2015**, *115*, 9277–9306. (b) Mahlau, M.; List, B. Asymmetric Counteranion-Directed Catalysis: Concept, Definition, and Applications. *Angew. Chem. Int. Ed.* **2013**, *52*, 518–533. (c) Brak, K.; Jacobsen, E. N. Asymmetric Ion-Pairing Catalysis. *Angew. Chem. Int. Ed.* **2013**, *52*, 534–561. (d) Kampen, D.; Reisinger, C. M.; List, B. Chiral Brønsted Acids for Asymmetric Organocatalysis. *Top. Curr. Chem.* **2010**, *291*, 395–456. (e) Akiyama, T. Stronger Brønsted Acids. *Chem. Rev.* **2007**, *107*, 5744–5758.
- (20) (a) Romanov-Michailidis, F.; Guéneé, L.; Alexakis, A. Enantioselective Organocatalytic Fluorination-Induced Wagner–Meerwein Rearrangement. *Angew. Chem. Int. Ed.* **2013**, *52*, 9266–9270. (b) Romanov-Michailidis, F.; Romanov-Michailidis, M.; Pupier, M.; Alexakis, A. Enantioselective Halogenative Semi-Pinacol Rearrangement: Extension of Substrate Scope and Mechanistic Investigations. *Chem. Eur. J.* **2015**, *21*, 5561–5583.
- (21) For some recent examples, see: (a) Kim, A.; Kim, A.; Park, S.; Kim, S.; Jo, H.; Ok, K. M.; Lee, S. K.; Song, J.; Kwon, Y. Catalytic and Enantioselective Control of the C–N Stereogenic Axis via the Pictet–Spengler Reaction. *Angew. Chem. Int. Ed.* **2021**, *60*, 12279–12283. (b) Proctor, R. S. J.; Chuentragool, P.; Colgan, A. C.; Phipps, R. J. Hydrogen Atom Transfer-Driven Enantioselective Minisci Reaction of Amides. *J. Am. Chem. Soc.* **2021**, *143*, 4928–4934. (c) Yang, B.; Dai, J.; Luo, Y.; Lau, K. K.; Lan, Y.; Shao, Z.; Zhao, Y. Desymmetrization of 1,3-Diones by Catalytic Enantioselective Condensation with Hydrazine. *J. Am. Chem. Soc.* **2021**, *143*, 4179–4186.

- (22) (a) Becke, A. D. *Phys. Rev. A* **1988**, *38*, 3098–3100. (b) Becke, A. D. *J. Chem. Phys.* **1993**, *98*, 5648–5652. (c) Lee, C.; Yang, W.; Parr, R. G. *Phys. Rev. B* **1988**, *37*, 785–789. (d) Hehre, W. J.; Radom, L.; P. v. R. Schleyer; Pople, J. A. *Ab Initio Molecular Orbital Theory*; John Wiley & Sons, Ltd: New York, 1986; Vol. 7.
- (23) Rappe, A. K.; Casewit C. J.; Colwell K. S.; Goddard, W. A.; Skiff, W. M.; *J. Am. Chem. Soc.* **1992**, *114*, 10024–10035.
- (24) (a) Liu, C.; Han, P.; Wua, X.; Tang, M. The Mechanism Investigation of Chiral Phosphoric Acid-Catalyzed Friedel–Crafts Reactions – How the Chiral Phosphoric Acid Regains the Proton. *Comput. Theor. Chem.* **2014**, *1050*, 39–45. (b) Reid, J. P.; Goodman, J. M. Transfer Hydrogenation of *ortho*-Hydroxybenzophenone Ketimines Catalysed by BINOL-Derived Phosphoric Acid Occurs by a 14-Membered Bifunctional Transition Structure. *Org. Biomol. Chem.* **2017**, *15*, 6943–6947. (c) Reid, J. P.; Goodman, J. M. Selecting Chiral BINOL-Derived Phosphoric Acid Catalysts: General Model To Identify Steric Features Essential for Enantioselectivity. *Chem. Eur. J.* **2017**, *23*, 14248–14260. (d) Shibata, Y.; Yamanaka, M. DFT Study of the Mechanism and Origin of Enantioselectivity in Chiral BINOL-Phosphoric Acid Catalyzed Transfer Hydrogenation of Ketimine and α -Imino Ester Using Benzothiazoline. *J. Org. Chem.* **2013**, *78*, 3731–3736. (e) Simón, L.; Goodman, J. M. Mechanism of BINOL-Phosphoric Acid-Catalyzed Strecker Reaction of Benzyl Imines. *J. Am. Chem. Soc.* **2009**, *131*, 4070–4077. (f) Hariharan, P. C.; Pople, J. A. The Influence of Polarization Functions on Molecular Orbital Hydrogenation Energies. *Theoret. Chim. Acta* **1973**, *28*, 213–222. (g) Hehre, W. J.; Ditchfield, R.; Pople, J. A. Self-Consistent Molecular Orbital Methods. XII. Further Extensions of Gaussian-Type Basis Sets for Use in Molecular Orbital Studies of Organic Molecules. *J. Chem. Phys.* **1972**, *56*, 2257–2261. (h) Luchini, G.; Alegre-Requena, J. V.; Funes-Ardoiz, I.; Paton, R. S. GoodVibes: Automated Thermochemistry for Heterogeneous Computational Chemistry Data [version 1; peer review: 2 approved with reservations]. *F1000 Research* **2020**, *9* (Chem Inf Sci), 291.
- (25) Frisch, M. J.; Trucks, G. W.; Schlegel, H. B.; Scuseria, G. E.; Robb, M. A.; Cheeseman, J. R.; Scalmani, G.; Barone, V.; Petersson, G. A.; Nakatsuji, H.; Li, X.; Caricato, M.; Marenich, A.; Bloino, J.; Janesko, B. G.; Gomperts, R.; Mennucci, B.; Hratchian, H. P.; Ortiz, J. V.; Izmaylov, A. F.; Sonnenberg, J. L.; Williams-Young, D.; Ding, F.; Lipparini, F.; Egidi, F.; Goings, J.; Peng, B.; Petrone, A.; Henderson, T.; Ranasinghe, D.; Zakrzewski, V. G.; Gao, J.; Rega, N.; Zheng, G.; Liang, W.; Hada, M.; Ehara, M.; Toyota, K.; Fukuda, R.; Hasegawa, J.; Ishida, M.; Nakajima, T.; Honda, Y.; Kitao, O.; Nakai, H.; Vreven, T.; Throssell, K.; Montgomery, J. A., Jr.; Peralta, J. E.; Ogliaro, F.; Bearpark, M.; Heyd, J. J.; Brothers, E.; Kudin, K. N.; Staroverov, V. N.; Keith, T.; Kobayashi, R.; Normand, J.; Raghavachari, K.; Rendell, A.; Burant, J. C.; Iyengar, S. S.; Tomasi, J.; Cossi, M.; Millam, J. M.; Klene, M.; Adamo, C.; Cammi, R.; Ochterski, J. W.; Martin, R. L.; Morokuma, K.; Farkas, O.; Foresman, J. B.; Fox, D. J. Gaussian 09, Revision D.01, Gaussian, Inc., Wallingford CT, 2016.
- (26) The research data supporting this publication can be accessed at <https://doi.org/10.17630/816af4fa-ef6a-4043-b0f9-b88f4f8a47f1>.
- (27) CCDC 1900850 (compound **20**) and 1900851 (compound **44**) contains the supplementary crystallographic data for this study. The data can be obtained free of charge from the Cambridge Crystallographic Data Centre via www.ccdc.cam.ac.uk/structures.

Table of Contents

